Progress In Electromagnetics Research B, Vol. 18, 243–257, 2009

A GENERAL FDTD ALGORITHM HANDLING THIN DISPERSIVE LAYER

B. Wei

Phyics Department
Xidian University
Xi'an, Shaanxi 710071, China

S.-Q. Zhang

Engineering College of CAPF
Xi'an, Shaanxi 710086, China

Y.-H. Dong and F. Wang

Phyics Department
Xidian University
Xi'an, Shaanxi 710071, China

Abstract—A novel general technique for treating electrically thin dispersive layer with the finite difference time domain (FDTD) method is introduced. The proposed model is based on the modifying of the node update equations to account for the layer, where the electric and magnetic flux densities are locally averaged in the FDTD grid. Then, based on the characteristics that the complex permittivity and permeability of three kinds of general dispersive medium models, i.e., Debye model, Lorentz model, Drude model, the permittivity and permeability can be formulated by rational polynomial fraction in $j\omega$; the conversion equation from frequency domain to time domain (i.e., $j\omega$ replaced by $\partial/\partial t$) and the shift operator method are then applied to obtain the constitutive relation at modified electrical points, and the time-domain recursive formulas for $\mathbf{D}$ and $\mathbf{E}$, $\mathbf{B}$ and $\mathbf{H}$ available for FDTD computation are obtained. Several numerical examples are presented, indicating that this scheme possesses advantages such as fine generalization, EMS memory and time step saving, and good precision.

Corresponding author: B. Wei (bwei@xidian.edu.cn).

1. INTRODUCTION

Many microwave devices contain electrically thin layer, and anechoic coatings used for shielding are also electrically small dispersive layer. Therefore, the numerical simulation of such electromagnetic problems is receiving much attention. The finite difference time-domain (FDTD) method has been widely used in electromagnetic field numerical algorithm [1–16] due to its excellent characteristics such as wide applicability, ability to deal with non-uniform media and capability to acquire wideband information with one time calculation combined with Fourier transformation. The electromagnetic problem containing thin layers can be solved basically in three ways: (1) To divide the volume into small enough cells. Although this is a rigorous technique, it is computationally extremely demanding, since very small cells are needed inside electrically dense objects to resolve the spatial variations of the electromagnetic fields. (2) Using the surface impedance boundary conditions (SIBCs), this method is usually employed to solve the problem concerning the perfect electric conductor (PEC) coating problem, but the implementation gets extremely complicated in the case of dispersive medium thin layer [3, 4]. (3) By locally modifying the iterative equations at nodes of the cells where the thin layer is located [5]. Considering the memory requirement and computational complication, we prefer the third approach, i.e., local modification to the iterative equations at the nodes of the cells in which the thin layer is located.

In dealing with the time-domain wideband computation, the problem of dispersive thin layers is much more complicated than that of non-dispersive thin layers. Such publications have seldom been seen in literature. In 2003 Mikko et al. [5] employed the node modification algorithm to deal with thin layer problem. In Mikko's work, the effective parameters at the modified nodes are obtained by weighed average method. In the mean time, some intermediate variables and many other parameters such as polarization intensity, current density, magnetization intensity and magnetic current density are required in the calculation. The derivative process is troublesome and complicated. In Mikko's algorithm the electric dispersion property of metal substrate thin dispersive layer is omitted, and only one-dimensional case of Lorentz medium is accounted for. Giulio Antonini et al. [6] utilized the surface impedance boundary conditions and Green's function method to treat the dispersive medium thin layer problem in free space, and again only one-dimensional numerical examples are given. As a whole, a disadvantage of the inhere algorithms is needed to deduce different formulations for unlike

dispersion model. In addition, only one-dimensional numerical examples are given; numerical examples concerning three-dimensional dispersive medium thin layer have not been seen.

In this paper, a general FDTD method modeling thin dispersive medium layer is proposed on the basis of references [5] and [7]. When the thickness of the electrically small dispersive thin layer is smaller than the dimension of the FDTD cell, the effective medium parameters at the modified points in the cells where the thin layer is located are found by utilizing weighted average to the electric flux densities and magnetic flux densities in the cell. Then, based on the characteristics of the complex permittivity and permeability of three kinds of general dispersive medium models, i.e., Debye model, Lorentz model, Drude model, the permittivity and permeability can be formulated by rational polynomial fraction in $j\omega$; the conversion equation from frequency domain to time domain (i.e., $j\omega$ is replaced by $\partial/\partial t$); the shift operator method are then applied to obtain the constitutive relation at modified electrical quantities; the time-domain recursive formulations for $\mathbf{D}$ and $\mathbf{E}$, $\mathbf{B}$ and $\mathbf{H}$ available for FDTD computation are obtained. The proposed scheme can deal with both electric and magnetic dispersive thin layer problems, making it easier for compiling the general three-dimensional program to treat the commonly-seen thin dispersive medium layer.

2. THE BASIC IDEAS OF NODE MODIFICATION ALGORITHM

The FDTD calculation is generally carried out by Yee cell as illustrated in Fig. 1(a). Bounded by the stability condition, it is impossible for the grids to be discretized too finely. FDTD can hardly handle the situation in which the thickness of the thin layer is smaller than the dimension of space discrete grid (as shown in Fig. 1(b)). In node modification algorithm, FDTD cell is categorized into two classes. One is ordinary cell in which the parameters of the electric and magnetic fields at the sampled points are set to the medium parameters of the cell (as shown in Fig. 1(a)). The other is modified cell (as shown in Fig. 1(b)) in which the effective medium parameters are required to simulate the contributions of thin layer.

From the analysis above, we can see that calculation of the effective medium parameters at nodes is one of the key problems in node modification algorithm. For non-dispersive medium, it is ok to substitute the effective parameters into the recursive formula directly. However, the parameters of dispersive medium vary with frequency, and the effective medium parameters also vary with frequency. Since

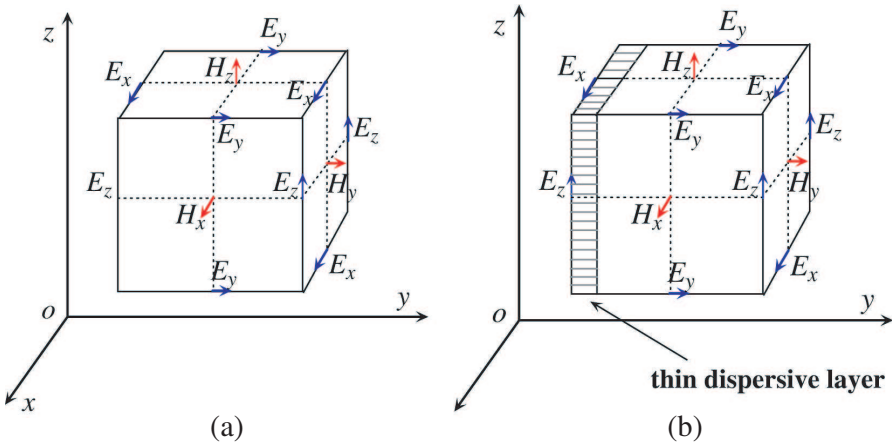

Figure 1. Yee Cell. (a) The ordinary case, (b) the case including thin dispersive layer.

FDTD calculation is performed in time-domain, it is required to obtain the time-domain recursive formula from the frequency-domain constitutive relation at the modified points. In the following sections, the way to acquire the effective medium parameters is introduced; the way to get the corresponding time-domain constitutive relation from frequency-domain constitutive relation is discussed; then the time-domain recursive formulas used for FDTD calculation are obtained.

3. THE EFFECTIVE COMPLEX PERMITTIVITY AND PERMEABILITY AT MODIFIED POINTS

In FDTD calculation, the modification of the nodes of electric field is associated with the effective complex permittivity, while the modification of the nodes of magnetic field is associated with the effective complex permeability. The calculation methods of the effective permittivity and permeability are given as follows:

(1) The thin dispersive layer in free space

If the thin dispersive layer is located in free space, and the thickness of the thin layer is smaller than the dimension of FDTD cell, the effective parameters at the modified points can be found by averaging the electric flux densities and magnetic flux densities in the cell. If the ratio of the volume of the thin layer inside the cell to that of the cell is α, the total electric flux density and magnetic flux density

can be represented by

$$\begin{aligned} \vec{D} &= \alpha\varepsilon_0\varepsilon_r(\omega)\vec{E} + (1-\alpha)\varepsilon_0\vec{E} \\ \vec{B} &= \alpha\mu_0\mu_r(\omega)\vec{H} + (1-\alpha)\mu_0\vec{H} \end{aligned} \tag{1}$$

Eq. (1) can be written as

$$\vec{D} = \varepsilon_0\varepsilon_{r,ave}\vec{E} \quad \vec{B} = \mu_0\mu_{r,ave}\vec{H} \tag{2}$$

where $\varepsilon_{r,ave}$, $\mu_{r,ave}$ are the effective relative permittivity and permeability at the modified points, respectively.

$$\varepsilon_{r,ave} = \alpha(\varepsilon_r - 1) + 1 \quad \mu_{r,ave} = \alpha(\mu_r - 1) + 1 \tag{3}$$

(2) Thin dispersive layer on the substrate of the PEC

For thin dispersive medium layer on the substrate of the perfect electric conductor, the effective parameters at the sampled points of the magnetic fields can also be obtained by local average method. However, the effects are not good enough if we use the same method to make node modification for the sampled points of electric fields [5]. The cross section chart in Fig. 1(b) perpendicular to PEC surface is shown as Figs. 2(a) and 2(b). Figs. 2(a) and 2(b) represent two cases in which the cell is incised along the edge and along the center of the cell, respectively (the double arrows in the figure stand for the points which need modification). The effective medium parameters at the modified points of the electric fields can be divided into two cases: (a) The effective medium parameters corresponding to the normal electric

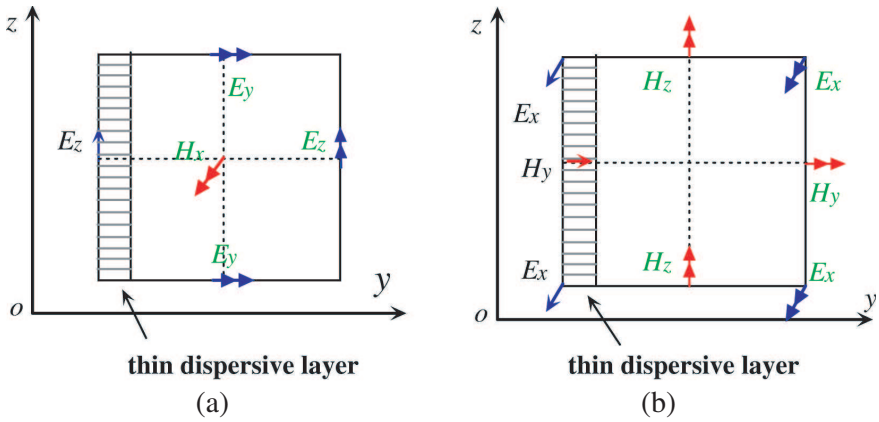

Figure 2. The modification of the tangential electric field strength near conductor surface. (a) The boundary surface separating two adjacent cells, (b) the central cross section of an Yee cell.

field on the surface (the y component of the electric field in Fig. 2) can still be obtained by the method mentioned in (1). (b) The effective parameters corresponding to the tangential electric field on the surface (the x and z components of the electric field in Fig. 2) can be obtained by the following method.

Assume that the thickness of the thin dispersive medium layer is d; spatial discrete size of the grid in y direction is Δy; $y = 0$ is the boundary surface separating the perfect electric conductor and dispersive medium. Obviously, the tangential electric field strength at $y = 0$ equals zero. We make an assumption that the tangential electric field behaves linearly in the range of $0 < y < 2\Delta y$ near the surface of the perfect electric conductor (x and z components of the electric field strength are shown in Figs. 1 and 2). Taking x component for example, we have

$$E_x(y) = \frac{y}{\Delta y} E_x|_1 \tag{4}$$

where $E_x(y)$ refers to the x component of the electric field strength near the perfect electric conductor. $E_x|_1$ is the x component of the electric field strength in the grid to the right of the surface of the conductor. The way to choose the effective parameters in the ranges of $0 < d \leq \Delta y/2$ and $\Delta y/2 < d < \Delta y$ is discussed as follows.

(1) If $0 < d \leq \Delta y/2$, we can find the effective relative permittivity at the modified points by averaging the electric flux densities in two individual cells which are located on the left and right sides of the modified points of the electric field strength near the surface of the conductors.

$$\begin{aligned} D_x|_1 &= \frac{1}{2\Delta y}\int_0^{2\Delta y} \varepsilon(y)\frac{y}{\Delta y} E_x|_1 \, dy \\ &= \frac{1}{2\Delta y}\int_0^{d} \varepsilon_0\varepsilon_r\frac{y}{\Delta y} E_x|_1 \, dy + \frac{1}{2\Delta y}\int_d^{2\Delta y} \varepsilon_0\frac{y}{\Delta y} E_x|_1 \, dy \\ &= \varepsilon_0\varepsilon_{r,ave} E_x|_1 \end{aligned} \tag{5}$$

where the effective complex relative permittivity can be written as

$$\varepsilon_{r,ave}(d,\varepsilon_r) = 1 + \frac{d^2}{4\Delta y^2}(\varepsilon_r - 1) \tag{6}$$

where ε_r is the relative permittivity of the dispersive medium.

(2) If $\Delta y/2 < d < \Delta y$, we can find the effective relative permittivity at the modified points by averaging the electric flux densities in two individual half cells which are located on the left and right sides of the modified points of the electric field strength near the

surface of the conductors.

$$\begin{aligned} D_x|_1 &= \frac{1}{\Delta y}\int_{\frac{\Delta y}{2}}^{\frac{3\Delta y}{2}} \varepsilon(z)\frac{y}{\Delta y}\, E_x|_1\, dy \\ &= \frac{1}{\Delta y}\int_{\frac{\Delta y}{2}}^{d} \varepsilon_0\varepsilon_r\frac{y}{\Delta y}\, E_x|_1\, dy + \frac{1}{\Delta y}\int_{y}^{\frac{3\Delta y}{2}} \varepsilon_0\frac{y}{\Delta y}\, E_x|_1\, dy \\ &= \varepsilon_0\varepsilon_{r,ave}(d,\varepsilon_r)\, E_x|_1 \end{aligned} \tag{7}$$

where the effective complex permittivity can be written as

$$\varepsilon_{r,ave}(d,\varepsilon_r) = \frac{9-\varepsilon_r}{8} + \frac{d^2}{2\Delta y^2}(\varepsilon_r - 1) \tag{8}$$

4. THE TIME-DOMAIN ITERATIVE FORMULATIONS AT THE MODIFIED POINTS

The effective permittivity and permeability of the dispersive medium are the function of frequency. In this case, the constitutive relation becomes convolution form in time domain, making it difficult to calculate the wave scattering and propagation in dispersive medium by FDTD. Problems concerning dispersive media can be solved by FDTD in several ways such as recursive convolution, Z transformation, current density convolution and auxiliary differential equation methods, etc. These methods lack generality since they are usually applied to different models for different dispersive media to obtain the corresponding recursive formulas. Next, we shall use FDTD combined with shift operator (SO-FDTD) [7] to give the time-domain recursive formulas for arbitrary dispersive medium models.

The formulas of the permittivity and permeability for three generic classes of linear isotropic dispersive media are as follows [11]:

(1) Debye model

$$\begin{aligned} \varepsilon(\omega) &= \varepsilon_\infty + \sum_{p=1}^{p}\frac{\varepsilon_{s,p}-\varepsilon_{\infty,p}}{1+j\omega\tau_{e,p}} \equiv \varepsilon_\infty + \sum_{p=1}^{p}\frac{\Delta\varepsilon_p}{1+j\omega\tau_{e,p}} \\ \mu(\omega) &= \mu_\infty + \sum_{p=1}^{p}\frac{\mu_{s,p}-\mu_{\infty,p}}{1+j\omega\tau_{m,p}} \equiv \mu_\infty + \sum_{p=1}^{p}\frac{\Delta\mu_p}{1+j\omega\tau_{m,p}} \end{aligned} \tag{9}$$

where $\Delta\varepsilon_p = \varepsilon_{s,p} - \varepsilon_{\infty,p}$, $\Delta\mu_p = \mu_{s,p} - \mu_{\infty,p}$, $\varepsilon_{s,p}$ and $\mu_{s,p}$ refer to the relative permittivity and relative permeability at static state or zero frequency, respectively. $\varepsilon_{\infty,p}$ and $\mu_{\infty,p}$ are the relative permittivity and relative permeability at infinitely large frequency, respectively;

$\tau_{e,p}$ and $\tau_{m,p}$ represent electric pole relaxation time and magnetic pole relaxation time, respectively.

(2) Lorentz model

$$\begin{aligned}\varepsilon(\omega) &= \varepsilon_\infty + \sum_{p=1}^{p} \frac{\Delta\varepsilon_p \omega_{e,p}^2}{\omega_{e,p}^2 + 2j\omega\delta_{e,p} - \omega^2} \\ \mu(\omega) &= \mu_\infty + \sum_{p=1}^{p} \frac{\Delta\mu_p \omega_{m,p}^2}{\omega_{m,p}^2 + 2j\omega\delta_{m,p} - \omega^2}\end{aligned} \tag{10}$$

where $\Delta\varepsilon_p$ and $\Delta\mu_p$ means the same as above; $\omega_{e,p}$ and $\omega_{\mu,p}$ are electric pole frequency and magnetic pole frequency, respectively; $\delta_{e,p}$ and $\delta_{m,p}$ are electric damping coefficient and magnetic damping coefficient, respectively.

(3) Drude model

$$\begin{aligned}\varepsilon(\omega) &= \varepsilon_\infty - \sum_{p=1}^{p} \frac{\omega_{e,p}^2}{\omega_{e,p}^2 - j\omega\gamma_{e,p}} \\ \mu(\omega) &= \mu_\infty - \sum_{p=1}^{p} \frac{\omega_{m,p}^2}{\omega_{m,p}^2 - j\omega\gamma_{m,p}}\end{aligned} \tag{11}$$

where $\omega_{e,p}$ and $\omega_{\mu,p}$ are frequencies of electric Drude pole and magnetic Drude pole, respectively; $\gamma_{e,p}$ and $\gamma_{m,p}$ are the reciprocal of the relaxation time of electric pole and magnetic pole, respectively.

It can be proved that the relative permittivity $\varepsilon_r(\omega)$ and relative permeability $\mu_r(\omega)$ in the above-mentioned three kinds of dispersive medium models can all be formulated by rational polynomial fraction in $j\omega$ [7]. Similarly, $\varepsilon_{r,ave}(\omega)$ and $\mu_{r,ave}(\omega)$ in Eqs. (3), (6) and (8) can also be formulated by rational polynomial fraction with respect to $j\omega$. That is

$$\begin{aligned}\varepsilon_{r,ave}(\omega) &= \left[\sum_{n=0}^{N} p_{ne}(j\omega)^n\right] \Bigg/ \left[\sum_{n=0}^{N} q_{ne}(j\omega)^n\right] \\ \mu_{r,ave}(\omega) &= \left[\sum_{n=0}^{N} p_{nm}(j\omega)^n\right] \Bigg/ \left[\sum_{n=0}^{N} q_{nm}(j\omega)^n\right]\end{aligned} \tag{12}$$

Here, the frequency-domain constitutive relations of dispersive medium

can be expressed as

$$\begin{aligned}\vec{D} &= \varepsilon_0 \left(\sum_{n=0}^{N} p_{ne} (j\omega)^n \Big/ \sum_{n=0}^{N} q_{ne} (j\omega)^n \right) \vec{E} \\ \vec{B} &= \mu_0 \left(\sum_{n=0}^{N} p_{nm} (j\omega)^n \Big/ \sum_{n=0}^{N} q_{nm} (j\omega)^n \right) \vec{H}\end{aligned} \tag{13}$$

Using the conversion equation from frequency domain to time domain, i.e., $j\omega$ replaced by $\partial/\partial t$, we can rewrite Eq. (13) as

$$\begin{aligned}\left[\sum_{n=0}^{N} q_{ne} (\partial/\partial t)^n \right] \vec{D} &= \varepsilon_0 \left[\sum_{n=0}^{N} p_{ne} (\partial/\partial t)^n \right] \vec{E} \\ \left[\sum_{n=0}^{N} q_{nm} (\partial/\partial t)^n \right] \vec{B} &= \mu_0 \left[\sum_{n=0}^{N} p_{nm} (\partial/\partial t)^n \right] \vec{H}\end{aligned} \tag{14}$$

Introducing the time-domain shift operator z_t defined by

$$z_t f^n = f^{n+1} \tag{15}$$

We can see that the function of the shift operator is to shift the value of the discrete time-domain array at time n to that at time $n+1$. It can be proved that [7] the shift operator of the partial derivative with respect to time can be written as

$$(\partial/\partial t)^n \quad \rightarrow \quad \{(2/\Delta t)\left[(z_t - 1)/(z_t + 1)\right]\}^n \tag{16}$$

Substituting Eq. (16) into Eq. (14) and putting it in order, we have the discrete time-domain constitutive relation (for simplicity, we set $h = 2\Delta t$, where Δt is the discrete time interval, and take x component as example)

$$\begin{aligned}\left[\sum_{l=0}^{N} q_{le} h^l (z_t+1)^{N-l} (z_t-1)^l \right] D_x^n &= \varepsilon_0 \left[\sum_{l=0}^{N} p_{le} h^l (z_t+1)^{N-l} (z_t-1)^l \right] E_x^n \\ \left[\sum_{l=0}^{N} q_{lm} h^l (z_t+1)^{N-l} (z_t-1)^l \right] B_x^n &= \varepsilon_0 \left[\sum_{l=0}^{N} p_{lm} h^l (z_t+1)^{N-l} (z_t-1)^l \right] H_x^n\end{aligned} \tag{17}$$

Eq. (17) is the discrete time-domain constitutive relation containing shifting operator at the modified points. Under ordinary conditions, we let N be 1 or 2 in engineering applications. For example, in the case of single pole Debye model, $N = 1$; in the cases of unmagnetized plasma, double pole Debye model, single pole Lorentz model and single pole Drude model, $N = 2$.

If $N = 2$, then we have the recursive equations from **D** to **E** and from **B** to **H** as follows:

$$\begin{aligned} E_x^{n+1} &= \left[a_{0e}\left(D_x^{n+1}/\varepsilon_0\right) + a_{1e}\left(D_x^n/\varepsilon_0\right) + a_{2e}\left(D_x^{n-1}/\varepsilon_0\right)\right. \\ &\quad \left. -b_{1e}E_x^n - b_{2e}E_x^{n-1}\right]/b_{0e} \\ H_x^{n+1} &= \left[a_{0m}\left(B_x^{n+1}/\varepsilon_0\right) + a_{1m}\left(B_x^n/\varepsilon_0\right) + a_{2m}\left(B_x^{n-1}/\varepsilon_0\right)\right. \\ &\quad \left. -b_{1m}H_x^n - b_{2m}H_x^{n-1}\right]/b_{0m} \end{aligned} \tag{18}$$

where

$$\begin{aligned} a_{0e} &= q_{0e} + q_{1e}h + q_{2e}h^2, & a_{1e} &= 2q_{0e} - 2q_{2e}h^2, \\ a_{2e} &= q_{0e} - q_{1e}h + q_{2e}h^2 & b_{0e} &= p_{0e} + p_{1e}h + p_{2e}h^2, \\ b_{1e} &= 2p_{0e} - 2p_{2e}h^2, & b_{2e} &= p_{0e} - p_{1e}h + p_{2e}h^2 \\ a_{0m} &= q_{0m} + q_{1m}h + q_{2m}h^2, & a_{1m} &= 2q_{0m} - 2q_{2m}h^2, \\ a_{2m} &= q_{0m} - q_{1m}h + q_{2m}h^2 & b_{0m} &= p_{0m} + p_{1m}h + p_{2m}h^2, \\ b_{1m} &= 2p_{0m} - 2p_{2m}h^2, & b_{2m} &= p_{0m} - p_{1m}h + p_{2m}h^2 \end{aligned} \tag{19}$$

For the general case of $N \geq 3$, Eq. (17) can be written as

$$\begin{aligned} E_x^{n+1} &= \frac{1}{b_{0e}}\left[\sum_{l=0}^{N} a_{le}\left(D_x^{n+1-l}\Big/\varepsilon_0\right) - \sum_{l=1}^{N} b_{le}E_x^{n+1-l}\right] \\ H_x^{n+1} &= \frac{1}{b_{0m}}\left[\sum_{l=0}^{N} a_{lm}\left(B_x^{n+1-l}\Big/\varepsilon_0\right) - \sum_{l=1}^{N} b_{lm}H_x^{n+1-l}\right] \end{aligned} \tag{20}$$

where a_{le}, b_{le} can be expressed by $q_{0e}, q_{1e}, \ldots q_{Ne}$, $p_{0e}, p_{1e}, \ldots p_{Ne}$, and a_{lm}, b_{lm} can be represented by $q_{0m}, q_{1m}, \ldots q_{Nm}$, $p_{0m}, p_{1m}, \ldots p_{Nm}$.

Equations (18) and (20) are the recursive equations of the electric and magnetic field strength at modified points as shown in Fig. 2.

5. NUMERICAL RESULTS

Example 1: The reflection coefficient of thin medium layer. The thin medium layer whose electric and magnetic parameters are both dispersive, parameters associated with permeability $\mu(\omega)$ are chosen as $\beta_{m,1} = 4 \cdot 10^{20}\,(\mathrm{rad/s})^2$, $\beta_{m,2} = 1.25 \cdot 10^{21}\,(\mathrm{rad/s})^2$, $\omega_{0m,1} = 5 \cdot 10^{10}\,(\mathrm{rad/s})$, $\omega_{0m,2} = 10 \cdot 10^{10}(\mathrm{rad/s})$, $\gamma_{m,1} = \gamma_{m,2} = 1$, $\delta_{m,1} = 5 \cdot 10^{9}\,(\mathrm{rad/s})$, $\delta_{m,2} = 4 \cdot 10^{9}\,(\mathrm{rad/s})$ and $\mu_\infty = 1$; Those for the permittivity $\varepsilon(\omega)$ are chosen as $\varepsilon_\infty = 2$, $\beta_{e,1} = 9 \cdot 10^{20}\,(\mathrm{rad/s})^2$, $\omega_{0e,1} = 3 \cdot 10^{10}\,(\mathrm{rad/s})$, $\gamma_{e,1} = 1$ and $\delta_{e,1} = 5 \cdot 10^{8}\,(\mathrm{rad/s})$. The size of FDTD spatial grid is 0.5 mm; the variation of the reflection coefficient with the frequency is shown in Fig. 3. Figs. 3(a) and 3(b) show the

cases that the thickness of the thin layer is equal to 0.4 mm and 0.2 mm, respectively. The circles in the figures correspond to the calculating results from the scheme in this paper, while the solid lines represent the analytical results. The calculating results are in good agreement with the analytical one.

Example 2: The reflection coefficient of thin Lorentz medium layer with metal substrate. The parameters of thin Lorentz medium layer and the size of FDTD spatial grid are the same as that of the above example. Figs. 4(a) and 4(b) represent the variation of the reflection coefficients of metal-backed thin dispersive layer with frequency for thickness of 0.4 mm and 0.2 mm, respectively. The circles in the figures

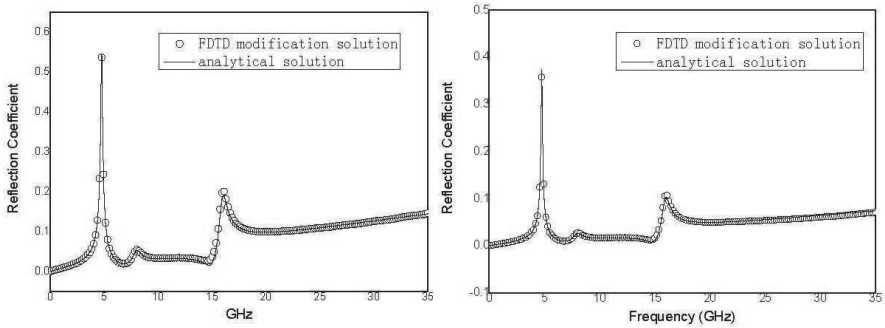

(a) d=0.4 mm (b) d=0.2 mm

Figure 3. Variation of reflection coefficients of thin Lorentz layer with frequency.

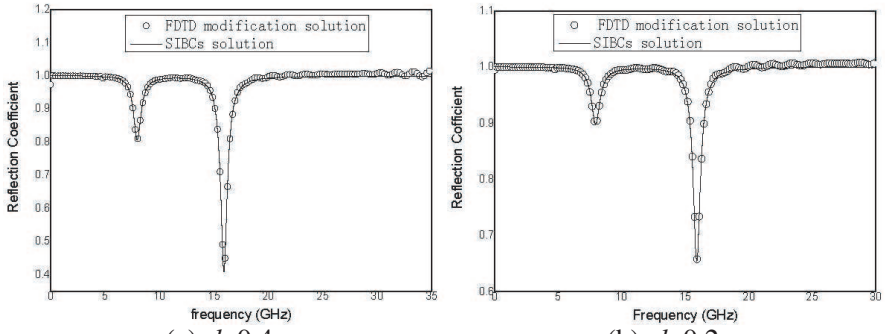

(a) d=0.4 mm (b) d=0.2 mm

Figure 4. Reflection coefficients of metal-backed thin Lorentz medium layer.

correspond to the calculated results from the scheme in this paper, while the solid lines represent the reflection coefficients calculated from the method of impedance boundary condition. Close agreement between these two types of results can be seen from the figures.

Example 3: The back scattering radar cross section (RCS) of a square metal plate coated with thin Lorentz medium layer. The side length and thickness of the metal plate are 100 mm and 5 mm, respectively. On one side of the plate is coated with thin dispersive layer. The electromagnetic wave normally incident on the side of the metal plate is coated with thin dispersive layer. The width of the cubic grid in FDTD is $\delta = 5$ mm; parameters of coating medium are $\beta_m = 4{\cdot}10^{20}\,(\mathrm{rad/s})^2$, $\omega_m = 2{\cdot}10^{10}\,(\mathrm{rad/s})$, $\delta_m = 5{\cdot}10^{9}\,(\mathrm{rad/s})$, $\gamma_m = 1$, $\mu_\infty = 1$, $\beta_e = 9 \cdot 10^{20}\,(\mathrm{rad/s})^2$, $\omega_e = 3 \cdot 10^{10}(\mathrm{rad/s})$, $\delta_e = 5 \cdot 10^{8}\,(\mathrm{rad/s})$, $\gamma_{e,1} = 1$ and $\varepsilon_\infty = 2$. Fig. 5 depicts the results of the back scattering RCS of the coated metal in different coating thicknesses. The circles and triangles in Fig. 5 represent the calculating results from node modification method when coating thicknesses are 2 mm and 4 mm, respectively. For comparison, the calculating results for smaller FDTD grid, 1 mm in this example, are also given. In this case the thickness of the thin layer is greater than the dimension of the cell, and the results can be regarded as the precise ones. The solid and dashed lines in Fig. 5 correspond to the calculated results when the FDTD grid dimension is 1 mm, and the thicknesses of the thin dispersive layer are 2 mm and 4 mm, respectively. Good agreement between these two types of results can be seen from the figure. It should be noted that the time required by modifying algorithm accounts for only 1/125 of that required by fine grid algorithm. The more is the number of the spatially discretized grid, the more time is required to accomplish

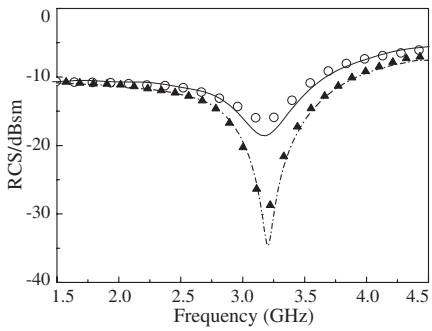

Figure 5. The back scattering RCS of a square metal plate coated with thin Lorentz medium layer.

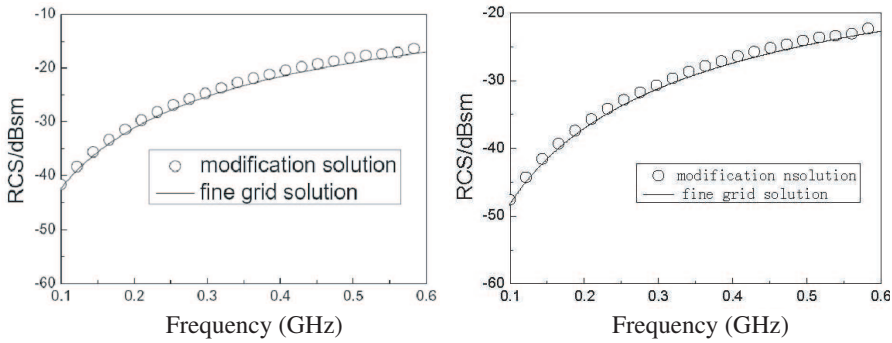

Figure 6. The back scattering RCS of thin dispersive plate of Debye model.

the computation. Therefore, the memory and time step saving are prominent using the modifying method in this paper.

Example 4: The back scattering RCS of thin dispersive plate of Debye model. A thin square dispersive plate is located in free space. The parameters of unmagnetized medium are: $\mu_r = 1.0$ and $\sigma_m = 0$, whose relative complex permittivity is the same as Eq. (9): $\varepsilon_s = 1.16$, $\varepsilon_\infty = 1.01$, $\sigma = 2.95 \times 10^{-4}\,\mathrm{S/m}$, $t_0 = 4.497 \times 10^{-10}\,\mathrm{s}$. The side length of the thin plate is 0.5 m. The size of FDTD grid is $\Delta x = \Delta y = \Delta z = 5\,\mathrm{cm}$, and time step is equal to $\Delta t = \Delta z/2c$. The electromagnetic wave is normally incident on the surface of the plate and is received in backward direction. Figs. 6(a) and 6(b) show the back scattering RCS of thin layer when the thicknesses are 4 cm and 2 cm, respectively. The circles in the figure correspond to the calculated results from the scheme in this paper, while the solid lines represent the reflection coefficients calculated from fine grid method (1 cm grid). Again, good agreement between these two cases can be seen from the figure. The memory consumption and computational time can be reduced by using modification method.

6. CONCLUSION

A local average method to the region where thin dispersive layer is located, and node modification algorithm for thin dispersive layer based on SO-FDTD are presented in this paper. Both the electric and magnetic dispersion cases can be handled by this scheme, realizing compiling one program to treat three types of commonly-met

medium targets in electromagnetic problems. Numerical results have demonstrated that the proposed scheme is of excellent computational precision, good generality, obvious EMS memory and computational time saving.

ACKNOWLEDGMENT

This project is supported by the National Natural Science Foundation of China (Grant No. 60871071) and the National Natural Science Foundation for Post-doctoral Scientist of China (Grant No. 20070421109).

REFERENCES

1. Yang, L. X., D. B. Ge, and B. Wei, "FDTD/TDPO hybrid approach for analysis of the EM scattering of combinative objects," *Progress In Electromagnetics Research*, PIER 76, 275–284, 2007.
2. Wang, M. Y., J. Xu, J. Wu, B. Wei, H.-L. Li, T. Xu, and D.-B. Ge, "FDTD study on wave propagation in layered structures with biaxial anisotropic metamaterials," *Progress In Electromagnetics Research*, PIER 81, 253–265, 2008.
3. Karkkainen, M. K., "FDTD model of electrically thick frequency-dispersive coatings on metals and semiconductors based on surface impedance boundary conditions," *IEEE Trans. Antennas Propagat.*, Vol. 53, 1174–1186, 2005.
4. Karkkainen, M. K., "FDTD surface impedance model for coated conductors," *IEEE Trans. EMC*, Vol. 46, 222–233, 2004.
5. Karkkainen, M. K., "Subcell FDTD modeling of electrically thin dispersive layers," *IEEE Transactions on MTT*, Vol. 51, 1774–1780, 2003.
6. Antonini, G. and A. Orlandi, "Time domain modeling of lossy and dispersive thin layers," *IEEE Microwave and Wireless Components Letters*, Vol. 17, 631–633, 2007.
7. Wei, B., D.-B. Ge, and F. Wang, "A general method for FDTD modeling of wave propagation in frequency-dispersive media," *Acta Phys. Sin.*, Vol. 57, 6290–6297, 2008 (in Chinese).
8. Maloney, J. G. and G. S. Smith, "The efficient modeling of thin material sheets in the finite-difference time-domain method," *IEEE Trans. Antennas Propagat.*, Vol. 40, 323–330, 1992.
9. Maloney, J. G., and G. S. Smith, "A comparison of methods for modeling electrically thin dielectric and conducting sheets in

the finite-difference time-domain (FDTD) method " *IEEE Trans. Antennas Propagat.*, Vol. 41, 690–694, 1993.

10. Tirkas, P. A., "Modeling of thin dielectric structures using the finite-difference time-domain technique," *IEEE Trans. Antennas Propagat.*, Vol. 39, 1338–1344, 1991.
11. Taflove, A., *Advances in Computational Electromagnetics: The FDTD Method*, 2nd edition, Artech House, Norwood, MA, 2005.
12. Hu, X.-J. and D.-B. Ge, "Study on conformal FDTD for electromagnetic scattering by targets with thin coating," *Progress In Electromagnetics Research*, PIER 79, 305–319,2008.
13. Hasar, U. C. and O. Simsek, "An accurate complex permittivity method for thin dielectric materials," *Progress In Electromagnetics Research*, PIER 91, 123–138, 2009.
14. Akerson, J. J., M. A. Tassoudji, Y. E. Yang, and J. A. Kong, "Finite difference time domain (FDTD) impedance boundary condition for thin finite conducting sheets," *Progress In Electromagnetics Research*, PIER 31, 1–30, 2001.
15. Gong, Z. and G.-Q. Zhu, "FDTD analysis of an anisotropically coated missile," *Progress In Electromagnetics Research*, PIER 64, 69–80, 2006.
16. Zheng, H.-X., X.-Q. Sheng, and E. K.-N. Yung, "Computation of scattering from anisotropically coated bodies using conformal FDTD," *Progress In Electromagnetics Research*, PIER 35, 287–297, 2002.